Article

Structural Insight into Guest Binding Sites in a Porous Homo-chiral Metal-Organic Material

Shi-Yuan Zhang, Lukasz Wojtas, and Michael J. Zaworotko

J. Am. Chem. Soc., **Just Accepted Manuscript** • DOI: 10.1021/jacs.5b06760 • Publication Date (Web): 07 Sep 2015

Structural Insight into Guest Binding Sites in a Porous Homochiral Metal-Organic Material

Shi-Yuan Zhang,[†,‡] Lukasz Wojtas, [‡] and Michael J. Zaworotko[*,†]

† Department of Chemistry, University of South Florida, 4202 East Fowler Avenue, CHE205, Tampa, Florida 33620, United States.

‡ Department of Chemical & Environmental Science, University of Limerick, Limerick, Republic of Ireland.

ABSTRACT: An enantiomeric pair of chiral metal-organic materials (CMOMs) based upon mandelate (man) and 4,4'-bipyridine (bpy) ligands, $[Co_2(S\text{-man})_2(bpy)_3](NO_3)_2\cdot$guest, (**1S·guest**) and $[Co_2(R\text{-man})_2(bpy)_3](NO_3)_2\cdot$guest, (**1R·guest**), has been prepared. The cationic frameworks exhibit 1D chiral channels with dimensions of 8.0 Å × 8.0 Å. The pore chemistry is such that chiral surfaces lined with nitrate anions and phenyl groups create multiple binding sites for guest and/or solvent molecules. The performance of **1S** and **1R** with respect to resolution of racemic mixtures of 1-phenyl-1-propanol (PP) was studied by varying time, temperature and the use of additives. Selectivity towards PP was determined by chiral HPLC with *ee* values of up to 60%. The binding sites and host-guest interactions were investigated through single crystal X-ray structural analysis of guest exchanged **1S** and **1R**. Crystallographically observed structural changes (e.g. absolute configuration of the three PP binding sites switch from *R*, *R* and *S* to *R*, *R* and *R*/*S*) correlate with experimentally observed *ee* values of 33% and 60% for variants of **1S** that contain PP and different solvent molecules, **1S·PPex** and **1S·PPex'**, respectively. That manipulation of guest solvent molecules, which in effect serve as cofactors, can modify chiral sites and increase enantioselectivity is likely to aid in the design of more effective CMOMs and processes for chiral separations.

1. INTRODUCTION

That metal-organic materials (MOMs)[1a] can exhibit permanent porosity has attracted considerable attention in the past 15 years.[1] An aspect of MOMs that exploits both their porosity and their fine-tunable chemical features is their ability to undergo guest exchange or be transformed by post-synthetic modification (PSM). For example, guest exchange enables MOMs to serve as "crystal sponges" for structure eludication[2] and chiral MOMs (CMOMs) have been studied in the context of enantioselective separation[3] and asymmetric catalysis[4]. PSM[5] can modify pore chemistry to enhance gas sorption performance[6] or can be used to access otherwise inaccessible MOMs.[7] The most typical approach to generate CMOMs involves homochiral molecular building blocks (CMBBs)[8] as opposed to relying upon spontaneous resolution of CMOMs sustained by achiral MBBs[9]. CMOMs with homochiral MBBs covalently bonded to the framework as linking or pendant ligands have been synthesized using a variety of ligands including L-aspartate[10], L-lactate[11], L-alanine derivatives[12], L-leucine derivatives[13], L-camphorate derivatives[14], D-tartrate derivatives[3c], BINOL derivatives[15] and Schiff base derivatives[16]. However, the relative cost of homochiral species and racemization during synthesis[17] has limited the development of CMOMs relative to MOMs in general[18]. Moreover, if there is a lack of control over pore chemistry, size and shape then chirality in a framework does not necessarily translate into binding sites that enable strong performance in the context of enantioselective separation. The benchmark performance is exhibited by M'MOF-7, which affords *ee* up to 82.4% for resolution of 1-phenylethanol.[16a] However, a hydrogen bonded network, HOF-2a, exhibits an *ee* of 92%.[15] In most instances much lower *ee* values are observed.[10-12,14]

Whereas the development of CMOMs in terms of network design and functionalization is well addressed,[13,19] the nature of the interactions that promote enantioselective separation by CMOMs is understudied. Simply put, the combination of porosity and chirality is not on its own enough to enable strong enantioselectivity. This is partly because of the dearth of single crystal X-ray structural studies of host-guest interactions in CMOMs since such studies require retention of crystallinity after guest exchange and crystallographically observable guest molecules[10,14]. Indeed, there are very few structural studies that reveal the intermolecular interactions between CMOMs and chiral guests[15,20]. Herein we report the synthesis and crystal structures of a pair of novel and robust CMOMs, $[Co_2(S\text{-man})_2(bpy)_3](NO_3)_2\cdot$guest (**1S·guest**) and $[Co_2(R\text{-man})_2(bpy)_3](NO_3)_2\cdot$guest (**1R·guest**). Our study reveals that relatively high *ee* values can be achieved through confined space that exploits the homochirality of the MBBs through van der Waal forces, hydrogen bonding interactions and π-π stacking interactions. Further, the role that solvent can play as a cofactor at binding sites is delineated.

2. EXPERIMENTAL SECTION

2.1. Materials and Synthesis: All reagents and solvents were commercially available and used as received.

2.1.1. Synthesis of **1S·NB** *and* **1R·NB**. A 5 mL methanol solution of 0.4 mmol $Co(NO_3)_2{\cdot}6H_2O$ (120 mg) and 0.4 mmol enantiopure mandelic acid (S isomer for **1S** and R isomer for **1R**, 60.8mg) was layered above a 5 mL nitrobenzene (NB) solution of 0.3 mmol bpy (46.8 mg). The buffer solution of a 5mL 1:1 methanol/nitrobenzene was layered between the top and the bottom layers to allow slow diffusion for 7 days. Red rectangular prismatic crystals were obtained in ~50% yield.

2.1.2. Synthesis of solvent exchanged variants **1S·guest** *and* **1R·guest**. Crystals of as-synthesized **1S·NB** and **1R·NB** were exchanged with DCM daily for 5 days affording **1S·DCM** and **1R·DCM**. Desolvated **1S** and **1R** were obtained from **1S·DCM** and **1R·DCM**, respectively, under vacuum. **1S·CH** and **1R·CH** were prepared by immersing crystals of **1S** and **1R** in cyclohexane (CH) for 7 days. Single crystals of **1S·PPex** were prepared by soaking **1S·DCM** in racemic PP for 7 days. Another variant, **1S·PPex'**, was prepared by soaking desolvated **1S** in racemic PP in the presence of 200 µL 90% $MeOH/H_2O$ for 5 days.

2.2. Characterization.

2.2.1. Physical measurements: Powder X-Ray diffraction was performed on a Bruker D8 Venture using Cu-Kα radiation (λ = 1.5418 Å). Thermogravimetric analysis was performed using a TA Instruments TGA-Q50 at a constant rate of 5ºC/min from 25ºC to 800ºC. UV-vis spectra were measured using a JASCO J-715. FT-IR spectra were recorded on a Perkin-Elmer Spectrum Two spectrometer. HPLC measurements were carried out on a Shimadzu HPLC system with Chiralcel OD-H column with a flow rate of 1 mL/min.

2.2.2. Crystallographic studies: As-synthesized **1S·NB** and **1R·NB**, guest exchanged **1S·CH, 1S·PPex** and **1S·PPex'** crystals are chosen for single crystal X-ray diffraction study. The data were collected on a Bruker D8 Venture PHOTON 100 CMOS system equipped with a Cu Kα INCOATEC Imus micro-focus source (λ = 1.54178 Å, *T* = 100(2) K). In all cases indexing was performed using APEX2.[21] Data integration and reduction were performed using SaintPlus 6.01.[22] Absorption correction was performed by multi-scan method implemented in SADABS.[23] Space groups were determined using XPREP implemented in APEX2. Structures were solved using Patterson Method (SHELXS-97), expanded using Fourier methods and refined on F^2 using nonlinear least-squares techniques with SHELXL-97 contained in APEX2 and WinGX v1.70.01[24-27] programs packages. Crystallographic data for the as-synthesized and guest exchanged CMOMs are summarized in Tables S1 and S2, respectively. Refinement details concerning the PP guest molecules are given in SI.

2.3. Chiral Resolution of PP.

The crystals used to study chiral resolution were obtained from layering and used as synthesized. **1S·DCM** and **1R·DCM** were immersed in 1 mL racemic PP with no stirring or shaking for various time periods and temperatures as detailed in Tables 1 and S3. Desolvated materials **1S** and **1R** were treated by a similar procedure except varying amounts of $MeOH/H_2O$ solutions were used as additives (Tables 2 and S4). After specific time periods, crystals were filtered and washed with CH (6 × 1 mL) to remove the residual PP from the surface of the crystals. DCM was then used to successively extract PP from the crystals (8 × 0.5 mL). The resulting extracts were monitored by TLC to ensure that all encapsulated PP had indeed been released. The filtrates were combined and analyzed by chiral HPLC to determine *ee* values and UV-vis was used to determine loading. The resulting crystals were dried in air and weighed (weights ranged from 0.03~0.04 g). A standard calibration curve for PP was generated (Scheme S1) and the following formula used to calculate the loading of PP: $\frac{experimental\ PP\ (mol)}{calculated\ PP\ (mol)} \times 100\%$. The chiral resolution procedure is expressed in the form of a flow chart in Scheme S2. HPLC data for the resolution of PP are presented in Figures S9-53.

3. RESULTS AND DISSCUSSION

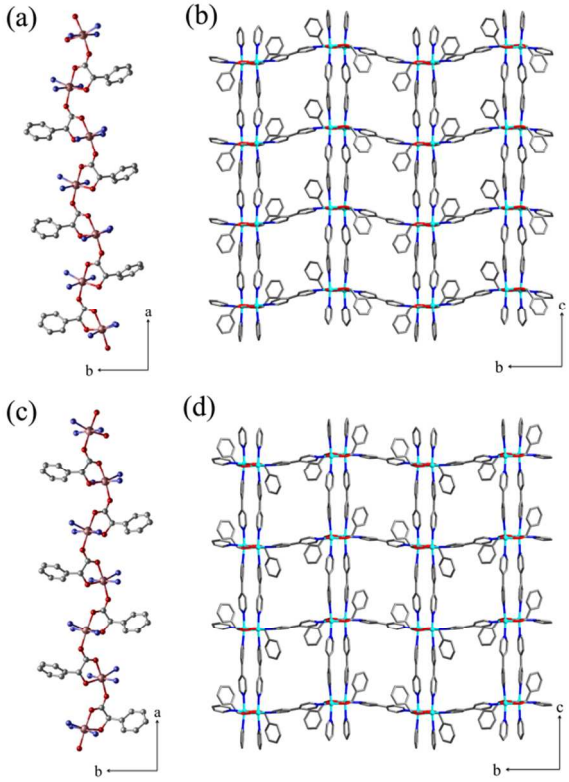

Figure 1. Left: The 1D chiral chains linked by (a) (*S*)-mandelate in **1S** and (c) (*R*)-mandelate in **1R**. Right: Projection of the structures of **1S** (b) and **1R** (d) from above the bc plane. Hydrogen atoms, nitrate anions and solvent molecules are omitted for the sake of clarity.

1S·NB and **1R·NB** were prepared by slow diffusion of a solution of $Co(NO_3)_2{\cdot}6H_2O$ and (*S*)-mandelic acid or (*R*)-mandelic acid, respectively, in MeOH onto 1:1 methanol/nitrobenzene that had been layered over a nitrobenzene solution of bpy. Single crystal X-ray diffraction analysis of **1S·NB** and **1R·NB** reveal that they are isostructural, crystallizing in chiral space group $P2_1$. The structure of **1S·NB** is sustained by Co^{2+} ions linked by (*S*)-mandelate anions so as to form 1D chiral chains running parallel to the *a* axis (Figure 1a). These chains are cross-linked by bpy linkers in the other two directions to form a 3D network with **bnn** topology (Figure 1b). In **1R·NB** the structure is of the opposite chirality (Figures 1c,d). The pore size of the 1D channels in **1S·NB** and **1R·NB** are defined by the length of bpy linkers (Figure S1): *ca.* 8.0 Å × 8.0 Å after subtracting van der Waals radii. Pore chemistry and

shape is controlled by the chiral mandelate linkers and nitrate counterions, resulting in uneven pore surfaces. The void volume of the pores was calculated using PLATON[21] to be 33% of the unit cell volume. The pores of the as-synthesized crystals of **1S·NB** and **1R·NB** are occupied by nitrobenzene. The positions and binding sites of NB inside the channels are shown and described in Figure S2.

We examined the ability of **1S·DCM** and **1R·DCM** to resolve 1-phenyl-1-propanol (PP) following procedures detailed in the experimental section. We selected PP for study because it is an important intermediate in the synthesis of pharmaceutical and parasiticide compounds.[3,28] PP exchanged **1S** materials were characterized by PXRD (Figure S4) and FT-IR (Figure S5). Table 1 reveals that **1S·DCM** and **1R·DCM** that had been soaked in racemic PP for 7d exhibit higher *ee* values, 32% and 30%, respectively, than samples exposed to PP for shorter time periods. The loading amount of PP was also observed to increase gradually, from 82% to 96%, within 5d. However, a further 2d of exposure resulted in decreased loading of PP. We attribute this effect to partial loss of crystallinity of the bulk sample as suggested by broadening of PXRD peaks (Figure S4). PP/additive exposed crystals also appeared to start losing crystallinity within 5 days. Conversely, PXRD profiles of **1S** soaked in CH were unchanged after one month (Figure S3). Thermogravimetric analysis (TGA) indicates that **1S** is stable to 200 °C (Figure S6). When resolution of PP was conducted at 40°C *ee* values remained ~26% from 1d to 5d (Table S3). However, the loading of PP started to decrease after only 3 days. These results indicate that 5 days at room temperature are optimal conditions for conducting separations since slow amorphization thereafter reduces loading.

Table 1. Resolution of PP by 1S·DCM and 1R·DCM at Room Temperature over Different Time Periods

CMOM	Time	(*S*)-PP:(*R*)-PP[a]	*ee* [%][a]	Loading [%][b]
1S·DCM	1d	41:59	18	82
	3d	39:61	22	88
	5d	39:61	22	96
	7d	34:66	32	70
1R·DCM	1d	58:42	16	83
	3d	61:39	22	88
	5d	62:38	24	97
	7d	65:35	30	71

[a] Determined by HPLC analysis using a chiral OD stationary phase. [b] Total amount of released PP was determined by UV-vis according to PP calibration curve.

To test the effect of additives upon performance, resolution experiments using **1S·DCM** and **1R·DCM** desolvated by vacuum were conducted. **1S** and **1R** were soaked in racemic PP in the presence of varying amounts of MeOH/H_2O at the optimal conditions found for pure PP, i.e. room temperature for 5 days. As detailed in Table 2, in the absence of MeOH/H_2O, *ee* values of 34% with loadings of 96% and 95%, respectively, were observed. Increasing MeOH/H_2O from 10 to 50 μL resulted in *ee* values remaining largely unchanged (~30% for **1S** and 38% for **1R**). However, the loading of PP decreased from 99% (98%) to 82% (86%) for **1S** (**1R**), indicating competition for the PP guest binding sites from MeOH/H_2O, accelerated amorphization or both. The highest *ee* value (60%) was observed with 200 μL of 90% methanol solution, but the loading was only 33%. Nevertheless, to our knowledge this performance is 1.7× higher than reported for any other porous MOM[12]. Further experiments were conducted at 40 °C for 1d (Table S4). The *ee* values were observed to improve gradually as the MeOH/H_2O ratio was increased. However, once again the loading of PP dropped, this time from 98% to 28%.

Table 2. Resolution of PP by 1S and 1R at Room Temperature for 5 days

CMOM[a]	Additive [μL, %][b]	(*S*)-PP: (*R*)-PP[c]	*ee* [%][c]	Loading [%][d]
1S	0, 0	33:67	34	96
	10, 50	30:70	40	99
	10, 90	35:65	30	97
	50, 50	35:65	30	83
	50, 90	34:66	32	82
	100, 90	25:75	50	72
	200, 90	20:80	60	33
1R	0, 0	67:33	34	95
	10, 50	69:31	38	98
	10, 90	69:31	38	97
	50, 50	69:31	38	86
	50, 90	69:31	38	86
	100, 90	72:28	46	70
	200, 90	76:24	52	30

[a] The desolvated material was obtained from **1S·DCM** and **1R·DCM** under vacuum. [b] Total volume (left) of an x% (right) MeOH aqueous solution (v/v) used as additive in 1 mL racemic PP. [c] Determined by HPLC analysis using a chiral OD stationary phase. [d] Total amount of released PP was determined by UV-vis according to a PP calibration curve.

That **1S** and **1R** retain crystallinity after solvent/guest exchange for at least several days enabled us to use single crystal X-ray crystallography to study the nature of the interactions between various guest molecules and the pore surfaces of **1S** and **1R**. For example, soaking crystals of **1S** in cyclohexane resulted in **1S·CH**, in which CH molecules lie in ordered positions and interact with phenyl groups and nitrate ions (Figure S7).

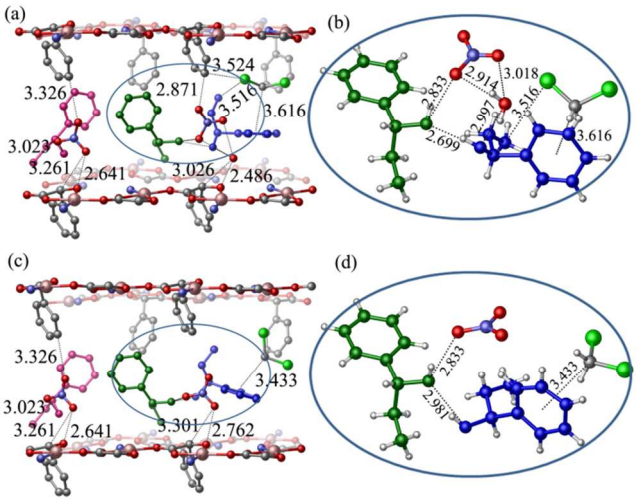

Figure 2. Locations of the three crystallographically independent PP molecules (colored magenta, green, and blue) in **1S·PPex**. The third PP molecule is disordered over two positions (a, b and c, d).

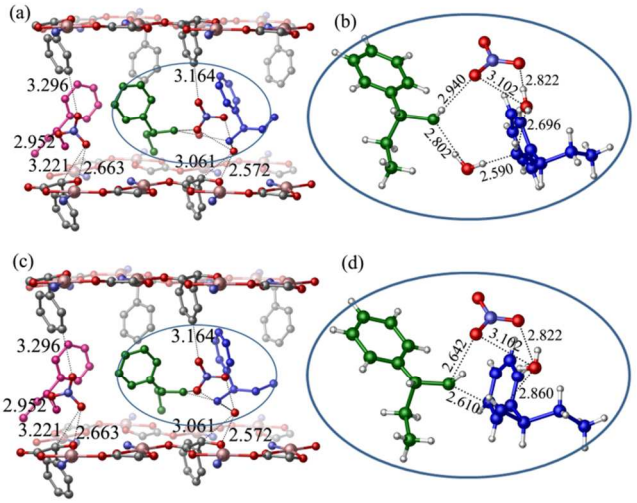

Figure 3. Locations of the three crystallographically independent PP molecules (colored magenta, green, and blue) in **1S·PPex'**. The second and the third PP molecules are disordered over two positions (a, b and c, d).

In order to better understand the enantioselectivity of **1S** towards racemic PP we also determined the single crystal structures of **1S·PPex** and **1S·PPex'**. The unit cells of **1S·PPex** and **1S·PPex'** are doubled those of **1S·NB** and **1S·CH**. Figures 2 and 3 provide insight as to why there is doubling of the unit cell and into why **1S-PPex** and **1S·PPex'** bind (*R*)-PP in preference to (*S*)-PP. There are three distinct PP binding sites. The first and second binding sites are similar. Specifically, hydroxyl groups from PP molecules form O-H···O hydrogen bonds with nitrate anions with contact distances of 3.023/2.833 Å and 2.934/2.892 (2.665) Å in **1S·PPex** and **1S·PPex'**, respectively. The most notable difference between the two structures is the direction, position and conformation of the third PP molecule. The third PP molecule is disordered over two positions as illustrated in Figures 2 and 3. In **1S·PPex**, a DCM molecule participates in a hydrogen bonded ring (Figure 2b) involving the nitrate anion, the second PP and the third PP. Additional close contacts between DCM and PP molecules with Cl···H-C_{ethyl} and C-H···π_{phenyl} distances of 3.516 and 3.616 Å occur. In the other disordered position (Figure 2d), the third PP interacts with the hydroxyl group of the second PP (O-H···O, 2.981 Å) and DCM (π···H-C, 3.433 Å) and results in it orienting nearly parallel with respect to the *bc* plane. The third PP molecule is resolved as the *R* enantiomer, meaning that the maximum *ee* value according to the crystal structure is 33% (a selectivity of 2:1 for (*R*)-PP over (*S*)-PP). In contrast, disordered water/methanol molecules in **1S·PPex'** participate in a cyclic hydrogen bonded ring (Figure 3b) involving a nitrate anion with the second and third PP molecules. This arrangement forces the third PP molecule to orient closer to perpendicular with respect to the *bc* plane. Figure 3d reveals that intermolecular hydrogen bonding interaction (C-H···O, 2.356 Å) between the second and the third PP molecules enables these PP molecules to lie in close proximity.

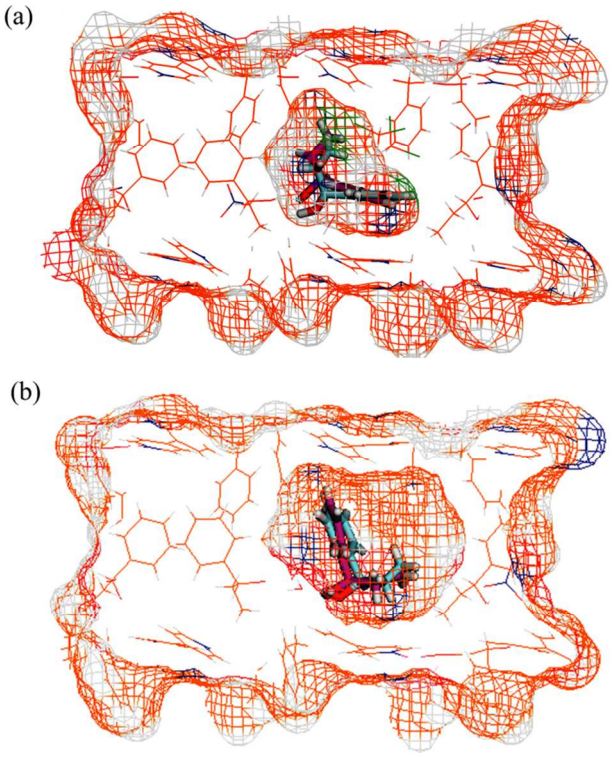

Figure 4. Perspective view of the binding sites occupied by the third PP molecule in **1S·PPex** (a) and **1S·PPex'** (b). The color of the mesh represents the element which generates the corresponding part of the surface. C orange, O red, N blue, Cl green, H white. The first and second binding sites are illustrated in Figure S8.

The change in orientation of the third PP could be responsible for the enantioselectivity for (*S*)-PP in **1S·PPex** relative to (*R*)-PP in **1S·PPex'**. Figures 4 illustrate that the binding sites are distinctly different even though most of the components around the binding site are unchanged.

Further, the hydroxyl groups of the third PP are fixed in both structures through hydrogen bonding to a nitrate anion and a water molecule. However, the DCM and water/methanol molecules in **1S·PPex** and **1S·PPex'**, respectively, profoundly impact the shape of the binding site. Specifically, the DCM molecule compresses the width of the cavity (Figure 4a) and prevents the phenyl group from aligning perpendicular to *bc* plane. Conversely, the water/methanol molecule reduces the length of the cavity (Figure 4b) and prevents the phenyl group from lying parallel to the *bc* plane. The overall effect of these structural changes is that there is higher enantioselectivity for the third PP in **1S·PPex'**. This effect is reminiscent of changing an enzyme's preference for cofactors.

1S·PPex' exhibits 60% *ee* for PP according to HPLC analysis but this is lower than expected from our crystallographic analysis. However, lower than expected *ee* values have also been observed by other groups,[10,29-30] presumably because of disorder of guest molecules in host channels. Gaining an understanding for the reasons for this lack of specificity of the chiral binding sites is necessary in order to design materials with even better *ee* performance.

4. CONCLUSION

We report the single step synthesis of a pair of robust CMOMs from commercially available chemicals. Thanks to the 1D homochiral channels within **1S** and **1R** enantioselective recognition towards PP was observed with *ee* values of up to 60%. Our study of the crystal structures of variants of **1S·PP** reveals how DCM and water/methanol molecules can play an important role in affecting the shape of the binding sites for PP. Indeed, the manipulation of guest solvent molecules, which in effect serve as cofactors, can be used to modify a PP binding site and increase the overall enantioselectivity. Further studies will be conducted to address the effect of pore size and pore chemistry upon enantioselectivity towards PP and other chiral guest molecules.

ASSOCIATED CONTENT

Supporting Information. Information of characterization data, supplementary schemes, tables and figures. This material is available free of charge via the Internet at http://pubs.acs.org.

AUTHOR INFORMATION

Corresponding Author

xtal@ul.ie

ACKNOWLEDGMENT

This work was supported by the U.S. Department of Energy (DE-AR0000177) and Science Foundation of Ireland for Award 13/RP/B2549. We thank Prof. Peter Zhang's group for their assistance with collection of HPLC data.

REFERENCES

(1) (a) Perry, J. J.; Perman, J. A.; Zaworotko, M. J. *Chem. Soc. Rev.* **2009**, 38, 1400. (b) Batten, S. R.; Neville, S. M.; Turner, D. R. *Coordination Polymers: Design, Analysis and Application; Royal Society of Chemistry: Cambridge*, U.K., **2009**. (c) MacGillivray, L. R. *Metal–Organic Frameworks: Design and Application*; John Wiley & Sons: Hoboken, NJ, **2010**.

(2) (a) Inokuma, Y.; Yoshioka, S.; Ariyoshi, J.; Arai, T.; Hitora, Y.; Takada, K.; Matsunaga, S.; Rissanen, K.; Fujita, M. *Nature* **2013,** *495,* 461. (b) Inokuma, Y.; Arai, T.; Fujita, M. *Nat. Chem.* **2010,** *2*, 780. (c) Fujita, D.; Suzuki, K.; Sato, S.; Yagi-Utsumi, M.; Yamaguchi, Y.; Mizuno, N.; Kumasaka, T.; Takata, M.; Noda, M.; Uchiyama, S.; Kato, K.; Fujita, M. *Nat. Commun.* **2012,** *3*, 1093.

(3) (a) Kim, K.; Banerjee, M.; Yoon, M.; Das, S. *Top. Curr. Chem*. **2010**, *293*, 115. (b) Liu, Y.; Xuan, W.; Cui, Y. *Adv. Mater,* **2010**, *22*, 4112. (c) Seo, J. S.; Whang, D.; Lee, H.; Jun, S. I.; Oh, J.; Jeon, Y. J.; Kim, K. *Nature* **2000**, *404*, 982.

(4) (a) Lee, J.; Farha, O. K.; Roberts, J.; Scheidt, K. A.; Nguyen, S. T.; Hupp, J. T. *Chem. Soc. Rev*. **2009**, *38*, 1450. (b) Yoon, M.; Srirambalaji, R.; Kim, K. *Chem. Rev*. **2011**, *112*, 1196.

(5) (a) Cohen, S. M. *Chem. Rev.* **2012**, *112*, 970. (b) Valtchev, V.; Majano, G.; Mintova, S.; Pérez-Ramírez, J. *Chem. Soc. Rev.* **2013**, *42*, 263. (c) Yoon, M.; Srirambalaji, R.; Kim, K. *Chem. Rev.* **2012**, *112*, 1196.

(6) (a) Tanabe, K. K.; Cohen, S. M. *Chem. Soc. Rev.* **2011**, *40*, 498. (b) Li, J.-R.; Ma, Y.; McCarthy, M. C.; Sculley, J.; Yu, J.; Jeong, H.-K.; Balbuena, P. B.; Zhou, H.-C. *Coord. Chem. Rev*. **2011**, *255*, 1791. (c) Mulfort, K. L.; Farha, O. K.; Stern, C. L.; Sarjeant, A. A.; Hupp, J. T. *J. Am. Chem. Soc.* **2009**, *131*, 3866.

(7) (a) Zhang, Z.; Zhang, L.; Wojtas, L.; Nugent, P.; Eddaoudi, M.; Zaworotko, M. J. *J. Am. Chem. Soc.* **2011,** *134*, 924. (b) Deria, P.; Mondloch, J. E.; Karagiaridi, O.; Bury, W.; Hupp, J. T.; Farha, O. K., *Chem. Soc. Rev.* **2014**, *43*, 5896.

(8) (a) Ma, L.; Abney, C.; Lin, W. *Chem. Soc. Rev*. **2009**, 38, 1248. (b) Anokhina, E.; Go, Y.; Lee, Y.; Vogt, T.; Jacobson, A. *J. Am. Chem. Soc.* **2006**, 128, 9957. (c) Morris, R.; Bu, X. *Nat. Chem*. **2010**, 2, 353. (d) Dybtsev, D. N.; Yutkin, M. P.; Peresypkina, E. V.; Virovets, A. V.; Serre, C.; Férey, G.; Fedin, V. P. *Inorg. Chem*. **2007**, 46, 6843.

(9) (a) Pérez-García, L.; Amabilino, D. *Chem. Soc. Rev.***2002**, 31, 342. (b) Biradha, K.; Seward, C.; Zaworotko, M. J. *Angew. Chem. Int. Ed.* **1999**, 38, 492. (c) Kepert, C. J.; Prior, T. J.; Rosseinsky, M. J. *J. Am. Chem. Soc.* **2000**, 122.

(10) Vaidhyanathan, R.; Bradshaw, D.; Rebilly, J.-N.; Barrio, J. P.; Gould, J. A.; Berry, N. G.; Rosseinsky, M. J. *Angew. Chem. Int. Ed.* **2006**, *45*, 6495.

(11) (a) Dybtsev, D. N.; Nuzhdin, A. L.; Chun, H.; Bryliakov, K. P.; Talsi, E. P.; Fedin, V. P.; Kim, K. *Angew. Chem. Int. Ed.* **2006**, *45*, 916. (b) Suh, K.; Yutkin, M. P.; Dybtsev, D. N.; Fedin, V. P.; Kim, K. *Chem. Commun.* **2012,** *48*, 513.

(12) Lin, L; Yu, R; Wu, XY; Yang, WB; Zhang, J. *Inorg. Chem.* **2014**, 53, 4794.

(13) Kuang, X.; Ma, Y.; Su, H.; Zhang, J.; Dong, Y.-B.; Tang, B. *Anal. Chem.* **2014**, *86*, 1277.

(14) Li, Z.-J.; Yao, J.; Tao, Q.; Jiang, L.; Lu, T.-B. *Inorg. Chem.* **2013**, 52, 11694.

(15) Li, P.; He, Y.; Guang, J.; Weng, L.; Zhao, J.; Xiang, S.; Chen, B. *J. Am. Chem. Soc.* **2014**, *136*, 547.

(16) (a) Das, M.; Guo, Q.; He, Y.; Kim, J.; Zhao, C.-G.; Hong, K.; Xiang, S.; Zhang, Z.; Thomas, K.; Krishna, R.; Chen, B. *J. Am. Chem. Soc.* **2012**, *134*, 8703. (b) Yuan, G.; Zhu, C.; Xuan, W.; Cui, Y. *Chem. Eur. J.* **2009**, *15*, 6428. (c) Li, G.; Yu, W.; Cui, Y. *J. Am. Chem. Soc.* **2008**, *130*, 4582.

(17) (a) Sang, R.-L.; Xu, L. *Chem. Commun.* **2013**, *49*, 8344. (b) Jhu, Z.-R.; Yang, C.-I.; Lee, G.-H. *CrystEngComm,* **2013**, *15*, 2456. (c) Liang, X.-Q.; Li, D.-P.; Li, C.-H.; Zhou, X.-H.; Li, Y.-Z.; Zuo, J.-L.; You, X.-Z. *Cryst. Growth Des*. **2010**, 10, 2596.

(18) (a) Li, J.-R.; Sculley, J.; Zhou, H.-C. *Chem. Rev*. **2012**, 112, 869. (b) Cook, T. R.; Yang, R.Y.; Stang, P. J.; *Chem. Rev*. **2013**, 113, 734.

(19) (a) Xuan, W.; Zhang, M.; Liu, Y.; Chen, Z.; Cui, Y. *J. Am. Chem. Soc.* **2012**, *134*, 6904. (b) Wang, W.; Dong, X.; Nan, J.; Jin, W.; Hu, Z.; Chen, Y.; Jiang, J. *Chem. Commun.* **2012**, *48*, 7022. (c) Zhang, M.; Pu, Z.-J.; Chen, X.-L.; Gong, X.-L.; Zhu, A.-X.; Yuan, L.-M. *Chem. Commun.* **2013**, 49, 5201. (d) Xie, S.-M.; Zhang, Z.-J.; Wang, Z.-Y.; Yuan, L.-M. *J. Am. Chem. Soc*. **2011**, 133, 11892. (e) Tanaka, K.; Muraoka, T.; Hirayama, D.; Ohnish, A. *Chem. Commun*. **2012**, 48, 8577.

(20) Jiang, J.; Babarao, R.; Hu, Z. *Chem. Soc. Rev*. **2011**, 40, 3599.

(21) Bruker, APEX2, **2010**, Bruker AXS Inc., Madison, Wisconsin, USA.

(22) Bruker, SAINT, **2009**, Data Reduction Software, Bruker AXS Inc., Madison, Wisconsin, USA.

(23) Sheldrick, G. M. SADABS, **2008**, University of Gottingen, Germany.

(24) Farrugia, L.J. *Appl. Crystallogr*. **1999,** 32, 837.

(25) Sheldrick, G.M. SHELXL-97, **1997**, Program for the Refinement of Crystal.

(26) Sheldrick, G.M. *Acta Cryst*. **1990**, A46, 467.

(27) Sheldrick, G. M. *Acta Cryst*. **2008**, A64, 112.

(28) (a) Wirth, T.; Kulicke, K. J.; Fragale, G. *J. Org. Chem.* **1996**, *61*, 2686. (b) Bagutski, V.; Elford, T. G.; Aggarwal, V. K. *Angew. Chem. Int. Ed.* **2011**, 50, 1080. (c) Chubb, N. A. L.; Cox, M. R.; Dauvergne, J. S.; Ewin, R. A.; Lauret, C. *U.S. Pat. Appl. Publ.* **2007**.

(29) Chen, L.; Reiss, P. S.; Chong, S. Y.; Holden, D.; Jelfs, K. E.; Hasell, T.; Little, M. A.; Kewley, A.; Briggs, M. E.; Stephenson, A.; Thomas, K. M.; Armstrong, J. A.; Bell, J.; Busto, J.; Noel, R.; Liu, J.; Strachan, D. M.; Thallapally, P. K.; Cooper, A. I. *Nat. Mater.* **2014**, *13*, 954.

(30) Dubbeldam, D.; Calero, S.; Vlugt, T. J. H. *Mol. Simul.* **2014**, *40*, 585.